Spleen tyrosine kinase functions as a tumor suppressor in melanoma cells by inducing senescence-like growth arrest

Olivier Bailet[1,3], Nina Fenouille[1,3], Patricia Abbe[1,3], Guillaume Robert[1,3], Stéphane Rocchi[1,3], Nadège Gonthier[2], Christophe Denoyelle[1,3], Michel Ticchioni[2,3], Jean-Paul Ortonne[1,4], Robert Ballotti[1,3,4], Marcel Deckert[2,3,5] and Sophie Tartare-Deckert[1,3,4*]

[1]INSERM, U895, Team 1, Biology and Pathologies of Melanocytes, Nice, France; [2]INSERM, U576, Nice, France; [3]University of Nice Sophia-Antipolis, Nice, France; [4]Department of Dermatology, CHU Nice, Nice, France and [5]Department of Clinical Hematology, CHU Nice, Nice, France.

[*]Corresponding author. Mailing address: INSERM U895, Faculté de Médecine, 28 avenue de Valombrose, 06107 Nice Cédex 2, France. Phone: (33) 493 377790. Fax: (33) 493 811404. E-mail: tartare@unice.fr

ABSTRACT

Loss of tumor suppressive pathways that control cellular senescence is a crucial step in malignant transformation. Spleen tyrosine kinase (Syk) is a cytoplasmic tyrosine kinase that has been recently implicated in tumor suppression of melanoma, a deadly skin cancer deriving from pigments-producing melanocytes. However, the mechanism by which Syk suppresses melanoma growth remains unclear. Here we report that re-expression of Syk in melanoma cells induces a p53-dependent expression of the cyclin-dependent kinase (cdk) inhibitor p21 and a senescence program. We first observed that Syk expression is lost in a subset of melanoma cell lines, primarily by DNA methylation–mediated gene silencing and restored after treatment with the demethylating agent 5-Aza-2-deoxycytidine. We analyzed the significance of epigenetic inactivation of Syk and found that reintroduction of Syk in melanoma cells dramatically reduces clonogenic survival and three-dimensional tumor spheroid growth and invasion. Remarkably, melanoma cells re-expressing Syk display hallmarks of senescent cells, including reduction of proliferative activity and DNA synthesis, large and flattened morphology, senescence-associated β-galactosidase activity and heterochromatic foci. This phenotype is accompanied with hypophosphorylated retinoblastoma protein (Rb) and accumulation of p21, which depends on functional p53. Our results highlight a new role for Syk tyrosine kinase in regulating cellular senescence and identify Syk-mediated senescence as a novel tumor suppressor pathway whose inactivation may contribute to melanoma tumorigenicity.

INTRODUCTION

Cutaneous melanoma is the leading cause of skin cancer-related mortality in Western societies owing to its high capability of invasion and rapid metastasis to other organs (1). The first step toward transition to melanoma is uncontrolled proliferation of epidermal melanocytes and dysplasia that may arise within a preexisting benign lesion (nevus) or more frequently directly from a new site. Subsequently, primary melanoma progresses through the radial growth phase (RGP) characterized by horizontal growth of transformed cells within the epidermis and the vertical growth phase (VGP), which is associated with depth invasion of cells into dermis and acquisition of metastatic potential (2). Melanoma formation and progression is accompanied by activating mutations in *B-RAF*, *N-RAS* and *KIT* genes as well as in *CDK4* gene and loss of tumor suppressor genes such as *CDKN2A*, *PTEN* and *E-cadherin* (2, 3). Oncogenic signaling and failure of tumor suppressor mechanisms are believed to contribute to the molecular pathogenesis of melanoma.

Cellular senescence represents a powerful tumor-suppressive process that constrains malignant transformation, as it controls excessive proliferation driven by oncogenic mutations (4-7). B-RAF mutations are the most prevalent oncogenic mutations in human melanocytic skin lesions (8). B-RAF^{V600E} mutation was found in

over two-thirds of human melanoma but also in a high proportion of benign nevi in which melanocytes were though to be senescent. Michaloglou *et al.* (9) demonstrated that B-RAF^{V600E} activates a senescence program that induces melanocyte growth arrest, and that senescence in nevus cells is triggered by B-RAF^{V600E} signaling. This work supports the model that nevi represent senescent clones of melanocytes and that senescence is a barrier to melanoma progression (10). In this context, senescence was shown to be dependent on p16^{INK4a} expression (11). The B-RAF^{V600E} study, however, has suggested that besides p16^{INK4a} another melanoma suppressor(s) contribute to protection against oncogenic B-RAF signaling (9). In this regard, the secreted protein IGFBP7 has been recently proposed to contribute to B-RAF^{V600E} - mediated cell senescence (12).

Spleen tyrosine kinase (Syk) is a nonreceptor tyrosine kinase that is widely expressed in hematopoietic cells. It contains tandem N-terminal Src homology 2 (SH2) domains, multiple tyrosine phosphorylation sites and a C-terminal tyrosine kinase domain. The SH2 domains bind phosphorylated immunoreceptor tyrosine-based activation motifs (ITAMs) and hence couple activated immunoreceptors to multiple downstream signaling pathways. Syk is essential for lymphocyte development and function, and signal transduction via a variety of membrane receptors in non-lymphoid cells such as mast cells or platelets (13). It was believed for years that Syk function was solely linked with hematopoietic cell signaling. However, more recent studies have indicated a ubiquitous pattern of *Syk* gene expression. Syk is expressed in endothelial cells, fibroblasts, epithelial cells and neuronal cells, but its function in these cells is not yet completely understood (14).

Accumulating evidence suggests that Syk can function as a tumor suppressor, unlike other tyrosine kinases that generally promote growth-stimulating activity leading to tumorigenicity (15). The role of Syk as candidate tumor suppressor has been well documented in breast cancer. Loss or reduced expression of Syk in human breast cancers was associated with a higher degree of malignancy and poor prognosis (16-18). Consistent with a role for Syk inactivation in tumor progression, re-expression of Syk in invasive breast cancer cells was shown to inhibit tumor growth and reduce metastasis in mouse xenografts (16). The tumor suppressive activity of Syk in breast cancer cells has been associated with abnormal mitotic progression and cell death (18, 19). Epigenetic silencing through hypermethylation of critical CpG islands was proposed to be involved in loss of Syk in a significant fraction of breast tumors (20). More recently, a similar loss of Syk expression has been documented in melanoma cells. Importantly, reintroduction of Syk was shown to restrict tumor growth and metastasis *in vivo* (21, 22). However, the molecular events responsible for Syk tumor suppressor effects in melanoma cells have remained completely unknown.

Here we aimed to investigate the tumor suppressor function of Syk in melanoma cells. We present evidence that Syk exerts its antitumor activity through induction of a senescence-like growth arrest and activation of a p53-dependent pathway, suggesting that loss of Syk may contribute to the senescence bypass generally observed in malignant melanoma. Our findings identify a novel link between the tyrosine kinase Syk, p53 and the senescent program in cancer cells.

MATERIALS AND METHODS

Reagents and plasmids

The list of antibodies used is provided in supplementary methods. Pifithrin-α (PFT-α) was from Calbiochem. p53 small interfering RNA (siRNA) was purchased from Santa Cruz Biotechnology. Wild-type and kinase-defective (Syk-KD, K395R) porcine Syk cDNAs as well as SH2 domains-deleted Syk mutant (Syk-ΔSH2) were cloned into pEF6/V5 vector. These mutants have been described elsewhere (23). The SH2-inactive domains mutant (Syk-SH2D) was produced using a QuikChange site-directed mutagenesis kit supplied by Stratagene. Recombinant adenoviruses expressing wild-type and kinase-defective Syk were kindly provided by Dr Yamamura (Kobe University Japan) and have been described previously (24).

Cell culture, RNAi, and adenovirus infection

Human melanoma cell lines were provided by Drs M. Herlyn (Wistar Institute, Philadelphia, PA) and F. Jotereau (INSERM U601, Nantes, France). Cells were routinely maintained in DMEM supplemented with 7% FBS as described elsewhere (25). Transfection of duplex siRNAs (50nM) was carried out using Lipofectamine RNAiMAX (Invitrogen). Adenovirus infection was performed as described previously (26).

Analysis of cell proliferation, colony formation assays and three-dimensional spheroid growth

For BrdU incorporation and DNA-content analysis, subconfluent cultures were pulsed with 10 μM BrdU for 4 hr. Cells were harvested and DNA stained with 7-amino-actinomycin D (7-AAD) and a APC-conjugated anti–BrdU antibody using the APC BrdU Flow Kit (BD Biosciences). Flow cytometric analyses were performed on a Becton Dickinson FACSCalibur machine and data were analysed using CellQuest software.

For colony formation assays, cells were transfected by using FuGENE 6 (Roche Diagnostics) with DNA mixtures containing 1 μg of the relevant plasmids plus 0.1 μg of pBabe-Puro vector. After 48 hr, cells were selected with 1 μg/ml of puromycin and maintained for 12-15 days. Colonies were fixed with 3% paraformaldehyde and stained with 0.4% crystal violet. The number of colonies was scored quantitatively using Image J software.

Melanoma spheroids were generated using the liquid overlay technique as described (27). Briefly, 24-well culture plates were coated with 1.5% agarose prepared in sterile water. Cells from a single-cell suspension were added at 10,000 per well. The plates were gently swirled and incubated at 37°C in 5% CO_2 atmosphere until spheroid aggregates were formed.

Senescence-associated β-galactosidase (SA-β-gal) staining

Cells were washed in PBS and fixed with 3% formaldehyde for 15 min at room temperature. Staining for SA-β-gal activity was performed as described previously

(28), utilizing the senescence β-galactosidase staining kit (Cell Signaling Technology). Stained cells were visualized by phase contrast microscopy, photographed and counted.

Immunoblotting and immunofluorescence

Whole cell lysates were prepared by lysing cells in radioimmunoprecipitation assay buffer supplemented with 1% NP40 and subjected to SDS-PAGE. Immunoblotting was accomplished according to standard procedures using enhanced chemiluminescence detection. For immunofluorescence, cells were fixed with 3% paraformaldehyde, and then incubated with primary and secondary antibodies as described elsewhere (25, 29).

Migration and invasion assays

Chemotaxis and Matrigel invasion assays were monitored using modified Boyden chambers as described (25, 29).

Statistical analysis

Unless indicated otherwise, experiments shown were representative of at least three independent experiments. Results were expressed as mean $\pm$ SD. Where appropriate the Student's t test was done and $P<0.001$ was considered statistically significant.

RESULTS

Syk expression and Syk promoter methylation status in melanocytes and melanoma cells

Initially, we examined expression, phosphorylation level and cellular localization of Syk in melanocytes. A 72 kDa band corresponding to Syk was readily detected by immunoblotting of lysates from different primary human melanocytes cultures (Supplementary Fig. S1). We also observed that Syk is phosphorylated on tyrosine 352, a site that has been proposed to bind signaling proteins (23, 30). Consistent with previous reports (21, 22), we observed that Syk is absent or nearly undetectable in most human primary and metastatic melanoma cells tested (Fig. S2). Methylation-specific PCR (MSP) studies showed that transcriptional silencing of Syk in Sbcl2, A375, 1205Lu and WM9 cells was associated with aberrant DNA methylation of the promoter region that we examined. In contrast, no methylation was observed for Syk-positive cell lines and melanocytes. However, we found that in Syk-negative WM793 cells, the promoter is unmethylated, suggesting that mechanism other than methylation of this region may be involved in *SYK* gene inactivation. Finally, we found that treatment with the demethylating drug, 5-azadC led to an increase of Syk mRNA levels whereas the histone deacetylase inhibitor TSA had no discernible effect on Syk mRNA expression (Fig. S2).

Syk decreases colony formation, tumor growth in 3D spheroids and chemotaxis

Having shown that Syk was inactivated in several melanoma cell lines, we examined its potential growth suppressor function in monolayer cultures and 3D spheroid

model. We transfected a Syk-expression plasmid into melanoma cell lines and colony formation assays were done to evaluate long-term growth on plastic dishes (Fig. 1A). Reintroduction of Syk dramatically reduced colony formation efficiency by at least 70% in Syk-negative A375 and SKmel28 cells. The same experiment was also carried out in 501mel cells expressing endogenous Syk protein levels (Fig. 1A, 501mel lanes; see Fig. S2 for Syk blot of 501mel showing endogenous Syk level). In this setting as well, elevated expression of Syk led to inhibition of colony formation. Transient transfection showed that each of the cell lines were able to express comparable levels of exogenous V5 epitope-tagged Syk (Fig. 1A).

We also investigated the effect of Syk reintroduction on tumor spheroid growth using adenoviral delivery system. To exclude the possibility that this effect would be the result of overexpression of Syk, we determined the level of Syk re-expression in melanoma cells and we found that level of exogenous Syk in lysates made from infected A375 cells was comparable to endogenous level seen in melanocytes (see supplemental information Fig. S3). In all subsequent experiments, we infected cells with a MOI of 5, which is the dose of virus that induces physiological level of Syk expression. Culture of WM793 cells under nonadherent conditions resulted in generation of 3D multicellular tumor spheroids, which may be used as an experimental model to study the tumor biology context. We prepared 3D spheroids from cells infected with control or Syk-expressing adenoviruses. After 3 days, there was significant decrease in spheroids diameter when cells were infected with Ad-Syk compared with vector control. Expression of adenovirus-delivered Syk was confirmed by immunoblot analysis (Fig. 1B). Together, these observations indicate

that Syk has growth-suppressing activity in standard monolayer cultures and 3D spheroids.

Finally, we analyzed the effect of Syk on melanoma cell migration and invasion towards serum using modified Boyden chambers assays. As seen Fig. 1C, re-expression of Syk markedly decreased A375 chemotactic migration and invasion. Because no further reduction was observed in the invasive capacity of cells, we can conclude that Syk primarily inhibits melanoma cell chemotaxis. Inhibition of tumor cell invasion into collagen I matrix by Syk was also evidenced in 3D cultures (Fig. S4).

Suppression of clonogenic survival by Syk is independent on functional SH2 domains but requires tyrosine kinase activity

Because A375 had complete methylation and silencing of Syk (Fig. S2) and was most sensitive to Syk-induced growth inhibition (Fig. 1A), we analyzed this cell line further. We conducted loss-of-function experiments, to define domain(s) of Syk that mediate growth suppression. We took advantage of a kinase-inactive mutant and generated a mutant that harbors inactivating mutations in the SH2 domains, as well as a mutant with a deletion of the two SH2 domains and interdomain A (Fig. 2A). Cells transfected with plasmids encoding these mutants or a wild-type control expressed similar levels of the corresponding proteins 3 days after transfection (Fig. 2B). Subsequently, these same transfections were subjected to colony-forming assay. As shown in Fig. 2C, expression of Syk SH2 mutants inhibited colony formation relative to vector control. Thus, Syk functions independently of its SH2 domains and

interdomain A to suppress colony formation abilities of melanoma cells. However, mutation of the ATP-binding site did not significantly inhibit the ability to form colonies, indicating that enzymatic activity of Syk is required for its effect on growth inhibition.

Expression of Syk inhibits proliferation by modulating cell cycle progression.

We undertook to determine how Syk reintroduction suppresses melanoma cell growth and survival. A375 were transduced with adenoviral vector expressing Syk and we analyzed ability of cells to proliferate by proliferation curves, cell cycle analysis and BrdU incorporation assays. Proliferation curves revealed that Syk re-expression markedly slowed growth of A375 cells (Fig. 3A). Levels of Syk expression in infected cells during the course of the experiment is shown Fig. 3B. We also examined cell cycle profiles of Syk-expressing and control cells 4 days after infection by flow cytometry (Fig. 3C). Restoration of Syk resulted in accumulation of cells in G0/G1 and decrease in S-phase cells compared with control cells, suggesting that Syk growth suppression results from G1 cell cycle arrest. In support of this, A375 cell population expressing Syk displayed a strong reduction in BrdU incorporation compared to vector-transduced cell population (Fig. 3D). Of note, cells transduced with Syk show no increase in sub-G1 phase and no caspase 3 activation, indicating that Syk expression did not result in cell death or apoptosis (Fig. 3A,C and data not shown).

Expression of Syk promotes senescence-like phenotypes

We observed that a major population of cells arrested by Syk displayed a flat

enlarged morphology with increased granularity that is characteristic of senescent cells (Fig. 4A). This increase in cell size was also observed by flow cytometry-based assays where Syk-expressing cells showed elevated side scatter that is characteristic of senescent cells. Senescence is accompanied by a series of genetic and metabolic changes that include accumulation of SA β-gal. To confirm that the observed morphological changes were due to induction of senescence, we assessed SA β-gal activity 6 days post-infection. A blue staining indicative of acidic β-gal activity was observed in the growth-arrested A375 infected with Ad-Syk (Fig. 4B). Notably, about 40% of cells were β-gal positive in Syk-expressing populations, whereas less than 2% of A375 cells were positive in vector-infected cultures (Fig. 4C). Lastly, we looked for the presence of senescence-associated heterochromatin foci (SAHF), another feature of senescent cells. Immunofluorescence analysis for HP1β, a marker of SAHF revealed punctuated regions of DNA corresponding to heterochromatic foci in Syk-expressing cells but not in control Syk negative cells (Fig. 4D). All together, these findings indicate that the cell-cycle arrest produced by Syk is mainly associated with induction of senescence-like phenotype.

Expression of Syk up-regulates the p53-signaling pathway

Next, we sought to understand the molecular payhway(s) involved in senescence-like growth arrest after Syk reintroduction. Immunoblot analysis was done to investigate expression and phosphorylation levels of specific proteins involved in cell cycle regulation. Increased levels of activating phosphorylation of p53 at Ser15 and induction of the cdk inhibitor p21 were observed in Syk-expressing A375 cells compared with controls (Fig. 5A). We also noticed that Syk expression resulted in

modest, but consistent, increase in the levels of total p53. In addition, Syk-expressing cells harbored dephosphorylation of pRb and lost cyclin A expression. Consistent with changes in p53 regulation, immunofluorescence of individual cells showed nuclear p53 accumulation in Syk-positive cells (Fig. 5B). The nuclear accumulation of p53 was similar to the one observed after treatment with the radio-mimicking drug bleomycin. These data indicate that Syk expression results in up-regulation of p53/p21 and pRb pathways, which are known to mediate cell-cycle arrest and premature senescence.

To substantiate further these observations, we analyzed by quantitative RT-PCR expression level of more than 90 transcripts involved in p53-dependent cell cycle regulation and survival following Syk re-expression (see supplemental information and Table S1). 29 genes appeared to be reproducibly modulated by Syk and some of them have been validated at protein level (Fig. 5A and Fig. S5). Among the 14 genes up-regulated, 6 were known transcriptional targets of p53 (*p21*, *Gadd45A*, *Reprimo*, *MDM2*, *BAX* and *SIVA*). DNMT-1 has been recently implicated in p53-dependent repression of Survivin, cdc2/cdk1 and mitotic cdc25C (31). Accordingly, these 3 genes were found repressed in Syk expressing cells as well as other repression targets of p53 such as *CHK1* and *Cyclins B*. Some relevant genes also down-regulated by Syk expression included *Livin*, *E2F1*, *BRCA1*, *Cyclins A2* and *E2* and *c-Myc*. Finally, we found that one of the genes deeply suppressed after Syk expression was *Caspase 2*, which is implicated in p53-mediated apoptosis (32). Inhibition of E2F1, Caspase 2 and survivin expression was confirmed at protein level (Fig. S5). Together, our results indicate that expression of Syk is linked to altered expression of essential cell

survival and cell cycle-regulatory genes that consequently results in G1 cell cycle arrest and inhibition of cell growth.

Inactivation of p53 prevents Syk-induced p21 expression

p21 is a well-characterized cdk inhibitor and a transcriptional target of p53 (33, 34). The p53/p21 axis plays a crucial role in mediating G1 arrest and senescence in normal and several tumor cells in response to multiple stress insults (4, 5). Our studies show that Syk-induced growth inhibition of melanoma cells is consistently associated with induction of this pathway. Therefore, we next investigated the requirement of p53 in Syk-induced p21 expression. To this end, A375 were incubated with the specific p53 inhibitor PFT-α (35). The level of p21 normally seen after Syk expression was significantly lower in PFT-α–treated cells than in control cells (Fig. 6A). Similarly, we observed that induction of p21 by bleomycin was partially suppressed in PFT-α–treated cells. To rule out the possible nonspecific effect of PFT-α, we used siRNA to inhibit p53 expression. Cells were transfected with p53-specific siRNA (or unrelevant control siRNA) and subsequently infected with adenovirus expressing Syk or empty vector as control. Fig. 6B shows that siRNA to p53 led to an efficient knockdown of p53 protein as well as p21 basal expression. This experiment also revealed that induction of p21 by Syk expression or bleomycin treatment was totally prevented in p53-silenced cells. These data indicate that p53 plays a functional role in mediating Syk-induced p21 expression. According to this, no induction of p21 was seen when Syk is expressed in MeWo cells, which have no functional p53 (Fig. 6C).

DISCUSSION

There is accumulating evidence that the Syk tyrosine kinase is a novel tumor suppressor in melanoma. However, its mechanism of action with respect to tumor suppression is not known. Here, we show that re-expression of Syk in melanoma cells at levels similar to that seen in melanocytes, results in suppression of chemotaxis, sustained cell cycle arrest, and senescence accompanied by molecular events associated with activation of the p53 tumor suppressor pathway. Our observations on the antiproliferative effect of Syk support the hypothesis that inactivation of *SYK* gene confers a specific growth advantage in neoplastic melanocyte cells and promotes migration of tumor cells. Together, our findings agree with recent observations showing that Syk expression in xenografted melanoma cells results in dramatic reduction of tumor growth and metastatic abilities (21, 22).

Consistent with a tumor suppressor function of Syk in melanoma, Syk levels are frequently low or undetectable in melanoma cells and primary tumors. The loss of expression occurs at transcriptional level, and, as a result of DNA hypermethylation (22). Our study identified a similar epigenetic regulation in the majority of melanoma cells analyzed. However, as shown in breast invasive tumors (18), our results suggested that mechanisms other than promoter methylation might account for loss of Syk expression in certain melanoma cells. Nevertheless, our results underscored a potential role of cytosine methylation in *SYK* gene inactivation in melanoma cells. It now remains to analyze the possible correlation between *SYK* methylation rate and clinicopathological parameters in melanoma tumors.

Inhibition of colony-forming activity by Syk provides a model system to study the mechanism by which Syk exerts its growth suppressive effect. We found that kinase activation of Syk and further downstream signaling are required for Syk-mediated inhibition of colony formation. In contrast, the SH2 domains of Syk are dispensable for the colony growth suppressive effect. This observation is consistent with the view that function of Syk in melanoma cells does not require the interaction of the SH2 domains with phosphorylated ITAM tyrosines on putative receptors or adaptor proteins. However, it is possible that Syk activity in melanoma depends on its subcellular localization. Reports have showed that repression of breast tumor cell growth by Syk is associated with its nuclear localization and transcriptional repressor function (36, 37). Also, loss of nuclear Syk expression was shown to be closely associated with the metastatic property of gastric cancer (38). Consistently, Zhou *et al*. (39) identified a shuttling sequence in Syk that accounts for its nucleocytoplasmic trafficking. It remains to be assessed whether such nuclear activity and localization of Syk occurs in melanoma cells and what are the structural element(s) of Syk involved in tumor suppression.

The growth suppression by Syk appears to be mediated through a G0/G1 cell cycle arrest and induction of senescence, and did not involve increased apoptosis or cell death. Interestingly, this activity seems specific to melanoma cells, as compared to breast carcinoma cells where expression of Syk triggered a non-apoptotic cell death through mitotic catastrophe (18, 19). This is consistent with the idea that Syk mediates senescence or death depending on the genetic background of the tumor. At this stage, the mechanism of tumor type-specific activity of Syk remains unclear.

p53 is a major regulator of cell-cycle arrest, senescence or apoptosis (40). Our findings provide the first evidence that tumor growth inhibition associated with Syk involves activation of p53 as reflected by phosphorylation of p53, nuclear accumulation and regulation of various p53-responsive genes. The net effect of these changes tips the balance in favor of proliferative arrest and protects cells from p53-dependent apoptosis. In support of this, expression of Caspase 2, a protease implicated in p53-mediated apoptosis (41, 32) was strongly suppressed following Syk re-expression. One of the major contributors of p53-directed cell cycle arrest and senescence is p21 (also known as senescent cell-derived inhibitor) (33, 41, 42), and we provide evidence for a functional requirement of p53 for p21 regulation by Syk. p21 functions by inhibiting cdk activity that results in hypophosphorylation of pRB and repression of E2F-targets genes, which blocks S phase entry and mediates cell cycle arrest. According to this, expression of Syk is consistently associated with hypophosphorylation of pRB and inhibition of E2F-targets genes such as cyclin A and cyclin B. Importantly, we also found a dramatic loss of E2F1 gene expression that can also account for the proliferative arrest and senescence experienced by melanoma cells expressing Syk. A similar down-regulation of E2F1 has been recently reported in senescing melanoma cells treated by the anticancer agent diperpene ester (43).

At present, we do not know the mechanism(s) through which Syk promotes phosphorylation and activation of p53. Phosphorylation of p53 may involve ATM/ATR DNA damage signaling pathways. However, it seems unlikely, as we did not observe activation of this pathway in cells expressing Syk (unpublished observations). The stress-activated c-jun N-terminal kinase might be a candidate for

the kinase that phosphorylates p53 (44). In this regard, it is interesting to note that Syk activates this pathway in melanoma cells (Fig. S6).

The results reported here might have important implications in our understanding of the physiological role of Syk in melanocytes. To date, the upstream signals involved in Syk activation and signaling pathways regulated by Syk in melanocytes are not known. However, because Syk modulates the p53 pathway in melanoma cells, we speculate that it may integrate p53-mediated stress responses in melanocytes. Accordingly, a link between Syk and oxidative stress signaling has been observed in B lymphocytes (39, 45). Like apoptosis, senescence is a stress response that prevents neoplastic transformation. Based on our observations, we propose that loss of Syk during melanoma development can lead to altered stress-dependent responses resulting in uncontrolled proliferation of abnormal cells. Additional investigations using suppression of Syk in melanocytes will elucidate how inactivation of Syk contributes to melanoma pathogenesis.

To conclude, our results uncover a novel role for Syk in regulation of p53 and senescence program, and give a molecular explanation for its tumor suppressive function in melanoma. This provides an important insight for further understanding tumorigenic and invasive processes, particularly in the context that epigenetic inactivation of Syk is associated with numerous cancers.

Acknowledgments

We thank H. Yamamura for Syk adenoviruses, M. Herlyn and F. Jotereau for melanoma cell lines. We also thank C. Gaggioli, G. Ponzio and R. Rottapel for helpful discussions.

Grant support: INSERM, ARC grant N° 3111 and INCa grant PL 2007.

O. Bailet is a recipient of an INSERM-région Provence Alpes Côte d'Azur PhD fellowship in partnership with Galderma R&D (Sophia -Antipolis, France).

S. Tartare-Deckert is a recipient of a Contrat d'Interface Clinique (CHU Nice).

REFERENCES

1. Chin L, Garraway LA, Fisher DE. Malignant melanoma: genetics and therapeutics in the genomic era. Genes Dev 2006;20:2149-82.

2. Miller AJ, Mihm MC, Jr. Melanoma. N Engl J Med 2006;355:51-65.

3. Curtin JA, Busam K, Pinkel D, Bastian BC. Somatic activation of KIT in distinct subtypes of melanoma. J Clin Oncol 2006;24:4340-6.

4. Campisi J. Senescent cells, tumor suppression, and organismal aging: good citizens, bad neighbors. Cell 2005;120:513-22.

5. Collado M, Serrano M. The senescent side of tumor suppression. Cell Cycle 2005;4:1722-4.

6. Serrano M, Lin AW, McCurrach ME, Beach D, Lowe SW. Oncogenic ras provokes premature cell senescence associated with accumulation of p53 and p16INK4a. Cell 1997;88:593-602.

7. Mooi WJ, Peeper DS. Oncogene-induced cell senescence--halting on the road to cancer. N Engl J Med 2006;355:1037-46.

8. Dhomen N, Marais R. New insight into BRAF mutations in cancer. Curr Opin Genet Dev 2007;17:31-9.

9. Michaloglou C, Vredeveld LC, Soengas MS, et al. BRAFE600-associated senescence-like cell cycle arrest of human naevi. Nature 2005;436:720-4.

10. Bennett DC. Human melanocyte senescence and melanoma susceptibility genes. Oncogene 2003;22:3063-9.

11. Gray-Schopfer VC, Cheong SC, Chong H, et al. Cellular senescence in naevi and immortalisation in melanoma: a role for p16? Br J Cancer 2006;95:496-505.

12. Wajapeyee N, Serra RW, Zhu X, Mahalingam M, Green MR. Oncogenic BRAF induces senescence and apoptosis through pathways mediated by the secreted protein IGFBP7. Cell 2008;132:363-74.

13. Turner M, Schweighoffer E, Colucci F, Di Santo JP, Tybulewicz VL. Tyrosine kinase SYK: essential functions for immunoreceptor signalling. Immunol Today 2000;21:148-54.

14. Yanagi S, Inatome R, Takano T, Yamamura H. Syk expression and novel function in a wide variety of tissues. Biochem Biophys Res Commun 2001;288:495-8.

15. Coopman PJ, Mueller SC. The Syk tyrosine kinase: A new negative regulator in tumor growth and progression. Cancer Lett 2006.

16. Coopman PJ, Do MT, Barth M, et al. The Syk tyrosine kinase suppresses malignant growth of human breast cancer cells. Nature 2000;406:742-7.

17. Toyama T, Iwase H, Yamashita H, et al. Reduced expression of the Syk gene is correlated with poor prognosis in human breast cancer. Cancer Lett 2003;189:97-102.

18. Moroni M, Soldatenkov V, Zhang L, et al. Progressive loss of Syk and abnormal proliferation in breast cancer cells. Cancer Res 2004;64:7346-54.

19. Zyss D, Montcourrier P, Vidal B, et al. The Syk tyrosine kinase localizes to the centrosomes and negatively affects mitotic progression. Cancer Res 2005;65:10872-80.

20. Yuan Y, Mendez R, Sahin A, Dai JL. Hypermethylation leads to silencing of the SYK gene in human breast cancer. Cancer Res 2001;61:5558-61.

21. Hoeller C, Thallinger C, Pratscher B, et al. The non-receptor-associated tyrosine kinase Syk is a regulator of metastatic behavior in human melanoma cells. J Invest Dermatol 2005;124:1293-9.

22. Muthusamy V, Duraisamy S, Bradbury CM, et al. Epigenetic silencing of novel tumor suppressors in malignant melanoma. Cancer Res 2006;66:11187-93.

23. Deckert M, Tartare-Deckert S, Couture C, Mustelin T, Altman A. Functionnal and physical interactions of syk family kinases with the vav proto-oncogene product. Immunity 1996;5:591-604.

24. Inatome R, Yanagi S, Takano T, Yamamura H. A critical role for Syk in endothelial cell proliferation and migration. Biochem Biophys Res Commun 2001;286:195-9.

25. Robert G, Gaggioli C, Bailet O, et al. SPARC represses E-cadherin and induces mesenchymal transition during melanoma development. Cancer Res 2006;66:7516-23.

26. Gaggioli C, Deckert M, Robert G, et al. HGF induces fibronectin matrix synthesis in melanoma cells through MAP kinase-dependent signaling pathway and induction of Egr-1. Oncogene 2005;24:1423-33.

27. Smalley KS, Haass NK, Brafford PA, Lioni M, Flaherty KT, Herlyn M. Multiple signaling pathways must be targeted to overcome drug resistance in cell lines derived from melanoma metastases. Mol Cancer Ther 2006;5:1136-44.

28. Dimri GP, Lee X, Basile G, et al. A biomarker that identifies senescent human cells in culture and in aging skin in vivo. Proc Natl Acad Sci U S A 1995;92:9363-7.

29. Gaggioli C, Robert G, Bertolotto C, et al. Tumor-derived fibronectin is involved in melanoma cell invasion and regulated by V600E B-Raf signaling pathway. J Invest Dermatol 2007;127:400-10.

30. Law CL, Chandran KA, Sidorenko SP, Clark EA. Phospholipase C-gamma1 interacts with conserved phosphotyrosyl residues in the linker region of Syk and is a substrate for Syk. Mol Cell Biol 1996;16:1305-15.

31. Esteve PO, Chin HG, Pradhan S. Human maintenance DNA (cytosine-5)-methyltransferase and p53 modulate expression of p53-repressed promoters. Proc Natl Acad Sci U S A 2005;102:1000-5.

32. Baptiste-Okoh N, Barsotti AM, Prives C. Caspase 2 is both required for p53-mediated apoptosis and downregulated by p53 in a p21-dependent manner. Cell Cycle 2008;7:1133-8.

33. el-Deiry WS, Tokino T, Velculescu VE, et al. WAF1, a potential mediator of p53 tumor suppression. Cell 1993;75:817-25.

34. Sherr CJ, Roberts JM. CDK inhibitors: positive and negative regulators of G1-phase progression. Genes Dev 1999;13:1501-12.

35. Komarov PG, Komarova EA, Kondratov RV, et al. A chemical inhibitor of p53 that protects mice from the side effects of cancer therapy. Science 1999;285:1733-7.

36. Wang L, Devarajan E, He J, Reddy SP, Dai JL. Transcription repressor activity of spleen tyrosine kinase mediates breast tumor suppression. Cancer Res 2005;65:10289-97.

37. Wang L, Duke L, Zhang PS, et al. Alternative splicing disrupts a nuclear localization signal in spleen tyrosine kinase that is required for invasion suppression in breast cancer. Cancer Res 2003;63:4724-30.

38. Nakashima H, Natsugoe S, Ishigami S, et al. Clinical significance of nuclear expression of spleen tyrosine kinase (Syk) in gastric cancer. Cancer Lett 2006;236:89-94.

39. Zhou F, Hu J, Ma H, Harrison ML, Geahlen RL. Nucleocytoplasmic trafficking of the Syk protein tyrosine kinase. Mol Cell Biol 2006;26:3478-91.

40. Vousden KH, Lane DP. p53 in health and disease. Nat Rev Mol Cell Biol 2007;8:275-83.

41. Chang BD, Watanabe K, Broude EV, et al. Effects of p21Waf1/Cip1/Sdi1 on cellular gene expression: implications for carcinogenesis, senescence, and age-related diseases. Proc Natl Acad Sci U S A 2000;97:4291-6.

42. Noda A, Ning Y, Venable SF, Pereira-Smith OM, Smith JR. Cloning of senescent cell-derived inhibitors of DNA synthesis using an expression screen. Exp Cell Res 1994;211:90-8.

43. Cozzi SJ, Parsons PG, Ogbourne SM, Pedley J, Boyle GM. Induction of senescence in diterpene ester-treated melanoma cells via protein kinase C-dependent hyperactivation of the mitogen-activated protein kinase pathway. Cancer Res 2006;66:10083-91.

44. Fogarty MP, Downer EJ, Campbell V. A role for c-Jun N-terminal kinase 1 (JNK1), but not JNK2, in the beta-amyloid-mediated stabilization of protein p53 and induction of the apoptotic cascade in cultured cortical neurons. Biochem J 2003;371:789-98.

45. Takano T, Sada K, Yamamura H. Role of protein-tyrosine kinase syk in oxidative stress signaling in B cells. Antioxid Redox Signal 2002;4:533-41.

LEGENDS TO FIGURES

Figure 1: *Reintroduction of Syk in melanoma cells abrogates colony formation, growth in 3D culture and migration.* (A) The indicated melanoma cell lines were transfected with a puromycin resistance vector and pEF-V5-wt-Syk expression vector or control empty vector (pEF). Stable puromycin-resistant colonies were stained and counted. Colony growth of cells transfected with control vector is normalized to 100% for each cell lines. *Columns*, mean of triplicate of a representative experiment; *bars*, SD. Representative plates are shown. A fraction of transfected cells was lysed and analyzed by immunoblotting for V5-tagged Syk expression. (B) Spheroids from WM793 cells infected with Syk-expressing (Ad-Syk) or empty vector adenoviruses were formed in liquid overlay cultures with agarose coat preventing cell adhesion to culture dishes. After 3 days, spheroids were viewed using a phase-contrast microscope and the diameter (μm) of at least 13 separate spheroids was determined. *, $P < 0.001$, Student's t test. Representative examples of spheroids are shown. Immunoblots show expression of Syk in spheroids transduced with control or with Syk-expressing adenoviruses. (C) Transwell migration and invasion assays of A375 infected with Syk-expressing or empty vector adenoviruses. The values are the mean $\pm$ SD of three independent experiments. *, $P < 0.01$, Student's t test.

Figure 2: *Syk suppresses colony growth independently of its two tandem SH2 domains.* (A) Functional domains of Syk and schematic of the mutants. (B) Control immunoblot shows expression of the V5-tagged Syk wt and mutants in transiently transfected

A375 cells. (C) Cells were transfected with empty vector (pEF), Syk wt, the SH2 deleted (ΔSH2), the SH2 mutated (SH2D) or the Kinase Dead (KD) Syk expression vector. Colony formation was analyzed as described in the legend of Fig.1. Representative plates are shown. *, $P < 0.001$, Student's *t* tests.

Figure 3: *Syk reduces the growth of melanoma cells and induces a G0/G1 cell cycle arrest.* (A) Proliferation curves of control and Syk-expressing cells. A375 cells were infected with control adenovirus or with adenoviruses expressing Syk for the indicated times. Result is from two independent experiments performed in triplicate, shown with SD. (B) Immunoblots of cellular lysates corresponding to cells transduced with control or with Syk-expressing adenoviruses. (C) Cell-cycle distribution of Syk-expressing and control populations as determined by BrdU incorporation and DNA-content flow cytometry analysis. Four days post-infection, cells were pulsed with BrdU and stained with anti-BrdU-APC to detect BrdU incorporation (vertical axis) and 7-AAD to detect total DNA (horizontal axis). The upper box indicates cells in S phase, the lower-left box identifies G0/G1 cells, and the lower-right box displays cells in G2/M. The percentage of cells in the different phases of the cell cycle is indicated. (D) Expression of Syk decreases S phase population. Percentage of BrdU positive cells in A375 transduced with control or Syk expressing adenoviruses. Data are mean $\pm$ SD of three separate experiments.

Figure 4: *Syk triggers senescence-like phenotypes.* (A) Phase-contrast images of A375 cells infected for 6 days with empty vector or with adenovirus encoding Syk. Syk-

transduced cells show a large and flat morphology with increased cytoplasmic granularity. The figure shown is a typical representation of the experiment that was performed at least five times (B) Induction of SA-β-gal activity in A375 cells by Syk. Cells were fixed and stained for SA-β-gal (pH 6.0) after 6 days of infection. Upper panels are low-magnification images and lower panels are high-magnification images. (C) Percentage of SA-β-gal-positive cells 7 days post-infection. At least 200 cells were scored from multiple randomly selected fields. Values represent the mean ± SD of three independent measurements. (D) Syk induces senescence-associated heterochromatin foci (SAHF). A375 cells were stained by immunofluorescence with anti-Syk (red) and anti-HP1β (green) 6 days post-infection and viewed under a fluorescence microscope. The percentage of SAHF positive cells is indicated in insert. Numbers given are representative of three independent experiments.

Figure 5: *Syk regulates expression and activity of senescence-associated markers.* (A) Lysates from A375 infected for 4 days with empty vector or with adenovirus encoding Syk were subjected to immunoblotting with the antibodies indicated on the left. (B) Immunofluorescent staining of vector- and Syk-expressing A375 cells. After 4 days of infection, cells were stained with anti-p53 antibody (green), anti-Syk antibody (red) or DAPI (blue). A treatment for 4 hr with bleomycin was used as positive control. Boxed regions correspond to larger magnifications of representative cells. The percentage of Syk-positive cells showing nuclear labeling of p53 is indicated in insert and is representative of three independent experiments.

Figure 6: *Induction of the cdk inhibitor p21 by Syk expression is p53 dependent.* (A) A375 cells infected with empty vector or with adenovirus encoding Syk for 2 days were incubated with pifithrin α (PFTα) (20 μg/ml) or DMSO as a vehicle control for additional 2 days. Cell lysates were tested for Syk, p53, Phospho (Ser15) p53, p21 and ERK2 by immunoblotting. (B) A375 cells were transfected with p53-siRNA or luciferase-siRNA (control). 6 hr later, cells were infected with empty vector or with adenovirus encoding Syk for 4 days. A treatment with bleomycin was used as positive control. Total cell lysates were subjected to immunoblotting analysis as in A). (C) MeWo (p53 defective) human melanoma cells were infected with empty vector or with adenovirus encoding Syk for 4 days. Cell lysates were tested for Syk, p53, p21 and ERK2 by immunoblotting.

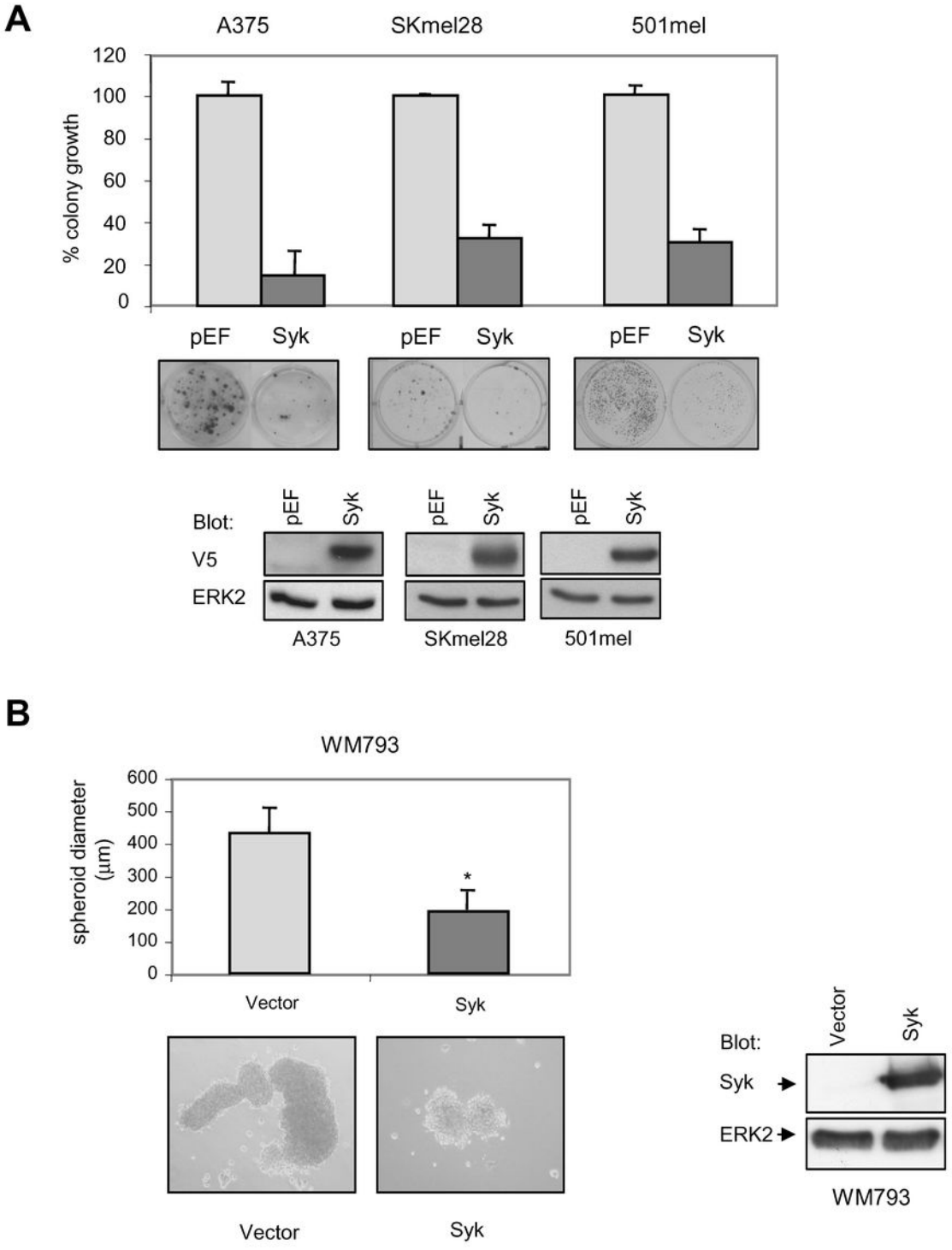
A
A375
SKmel28
501mel
% colony growth
120
100
80
60
40
20
0
pEF
Syk
pEF
Syk
pEF
Syk
Blot:
V5
ERK2
pEF
Syk
pEF
Syk
pEF
Syk
A375
SKmel28
501mel
B
WM793
spheroid diameter (µm)
600
500
400
300
200
100
0
*
Vector
Syk
Vector
Syk
Blot:
Syk
ERK2
Vector
Syk
WM793

Figure 1

C

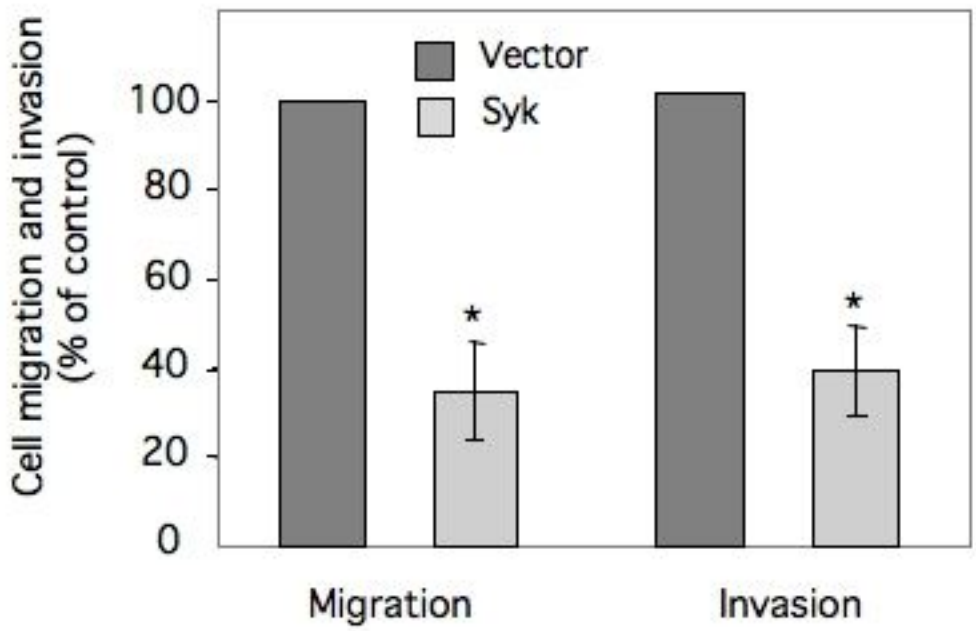
Cell migration and invasion
(% of control)
100
80
60
40
20
0
Vector
Syk
*
*
Migration
Invasion

Figure 1

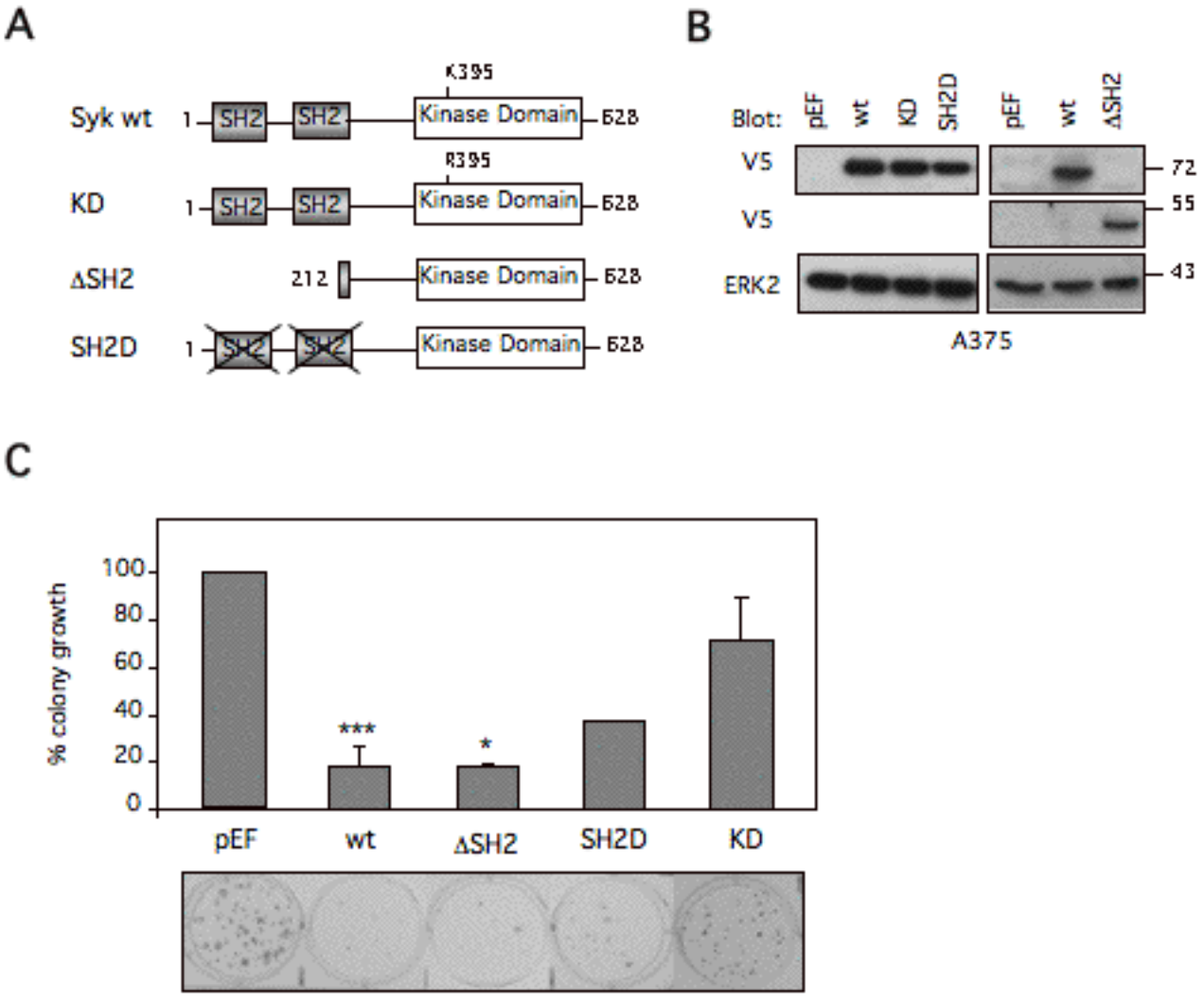
A
Syk wt
KD
ΔSH2
SH2D
SH2
Kinase Domain
628
212
B
Blot:
pEF
wt
KD
SH2D
ΔSH2
V5
ERK2
72
55
43
A375
C
% colony growth
100
80
60
40
20
0
***
*
pEF
wt
ΔSH2
SH2D
KD

Figure 2

A

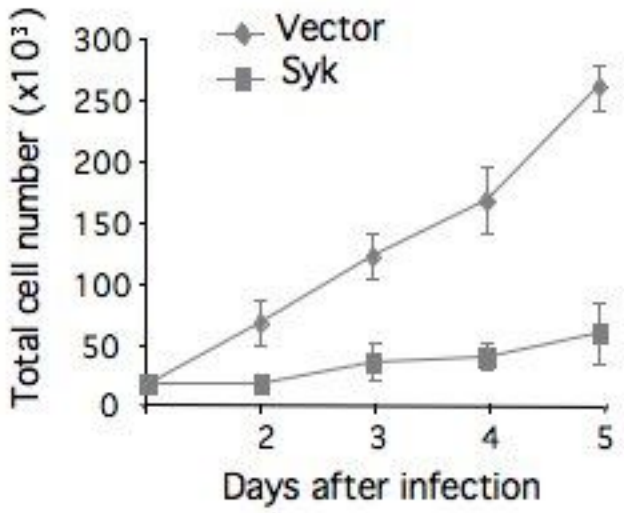

B

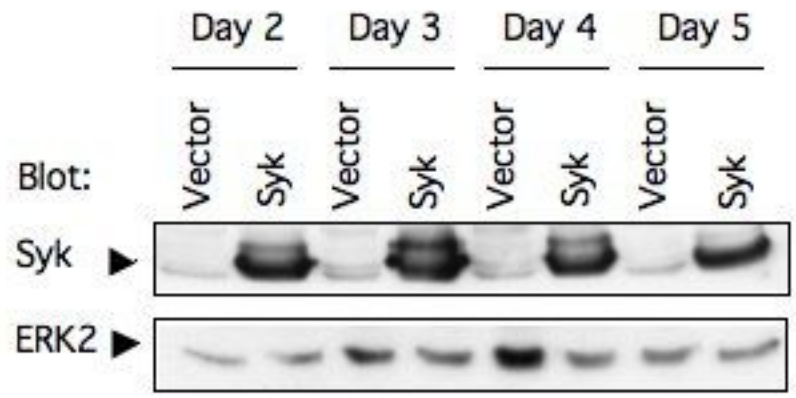

C

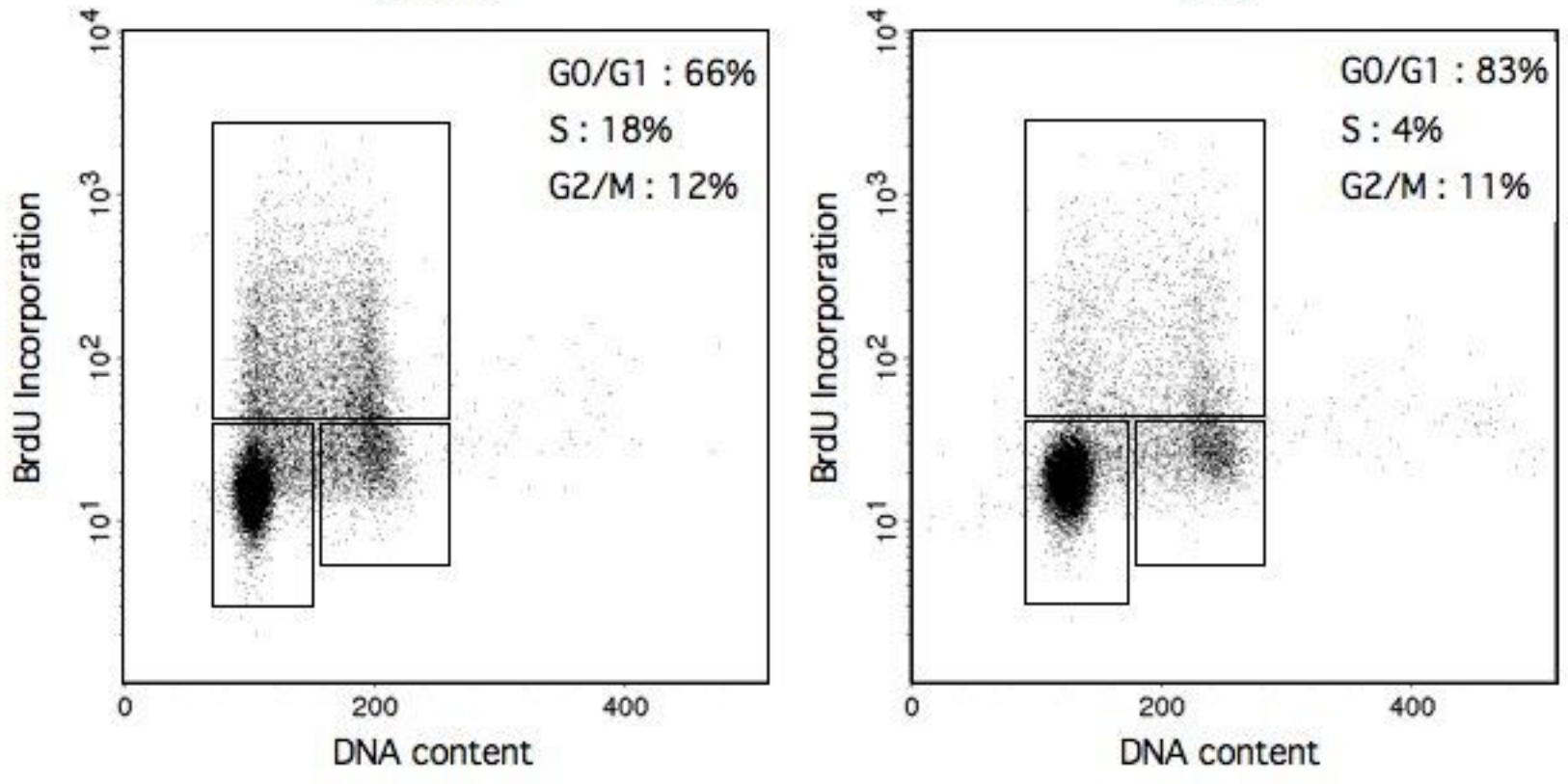

D

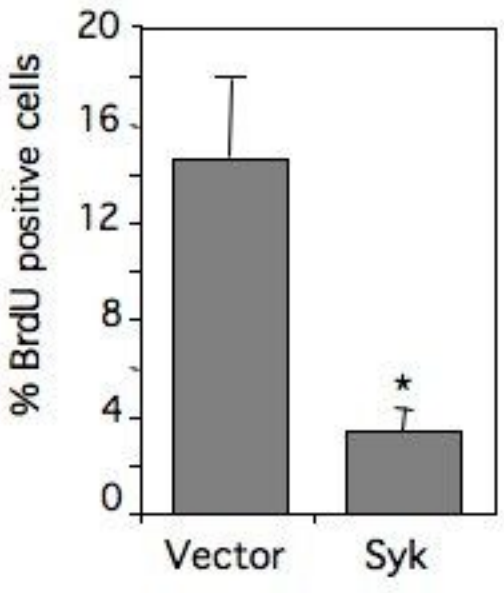

Figure 3

A

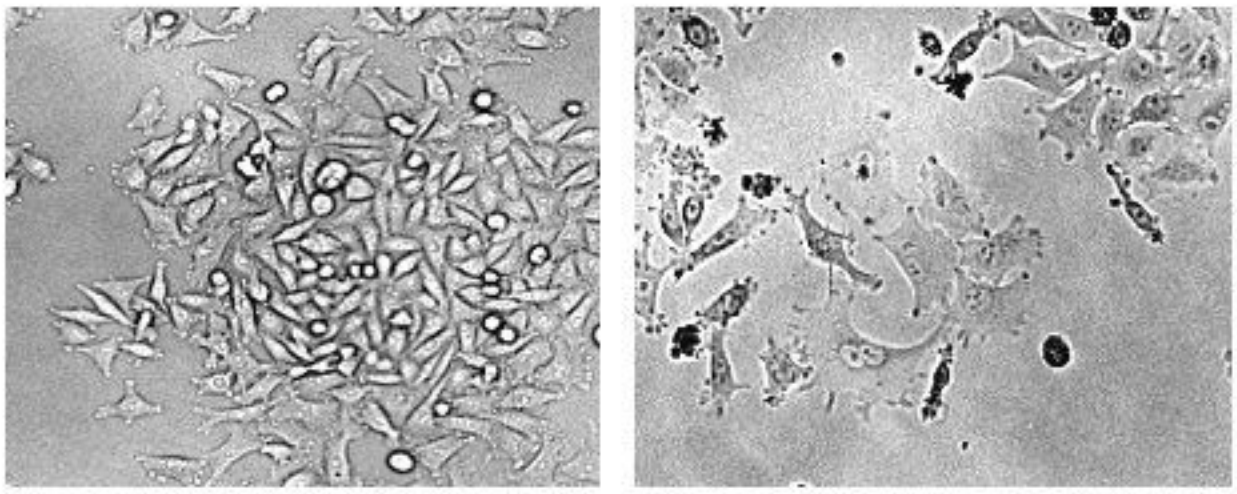

B

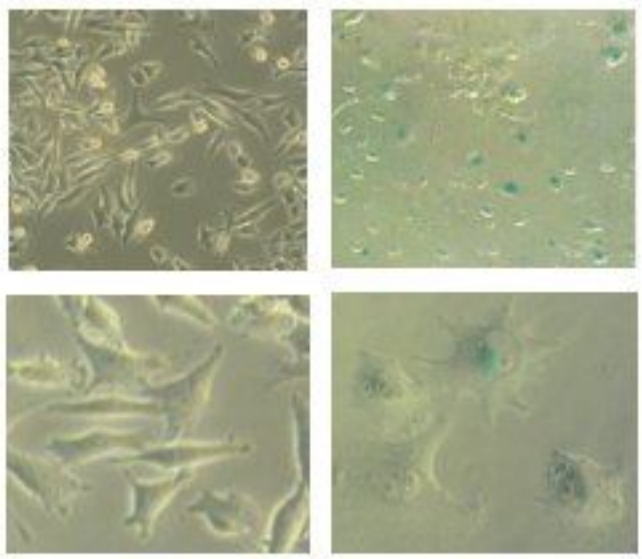

SA-β-galactosidase staining

C

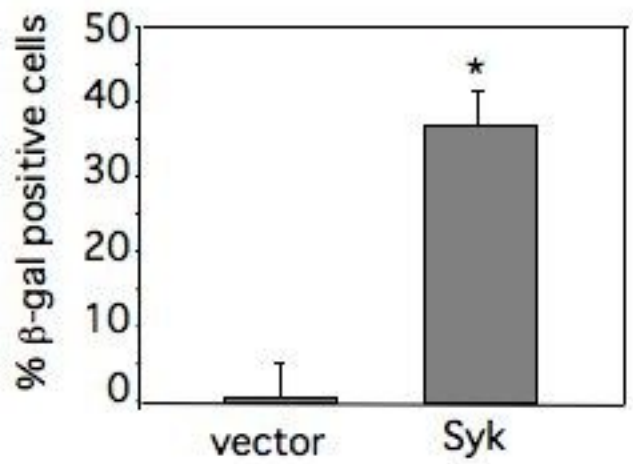

D

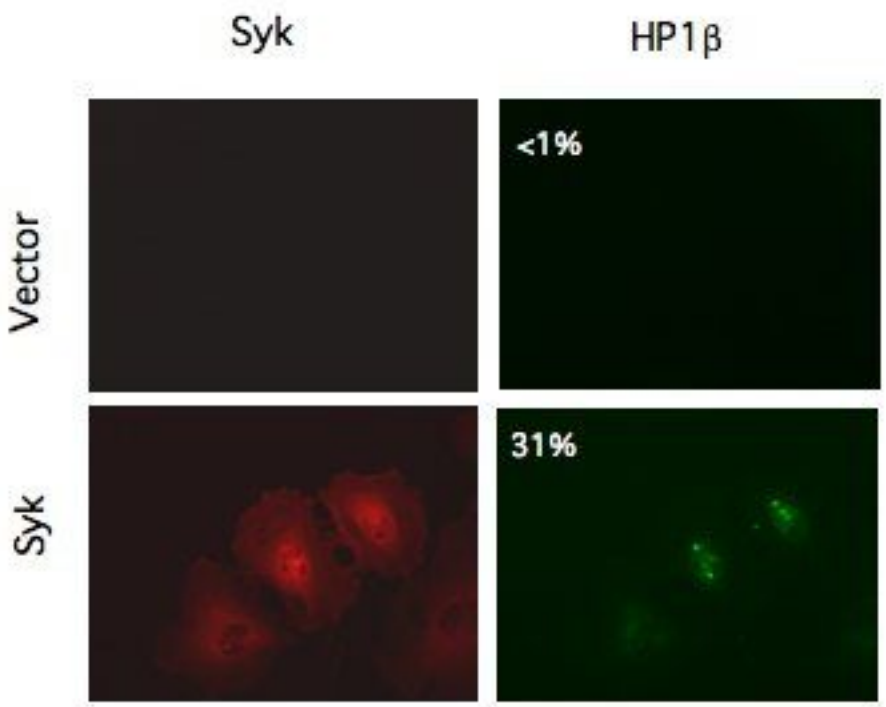

Figure 4

A

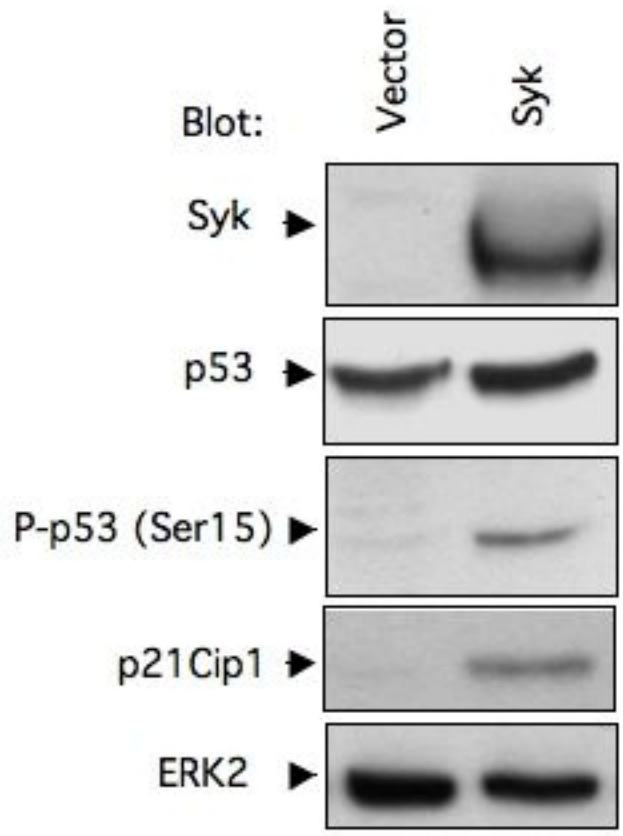
Blot:
Vector
Syk
Syk
p53
P-p53 (Ser15)
p21Cip1
ERK2

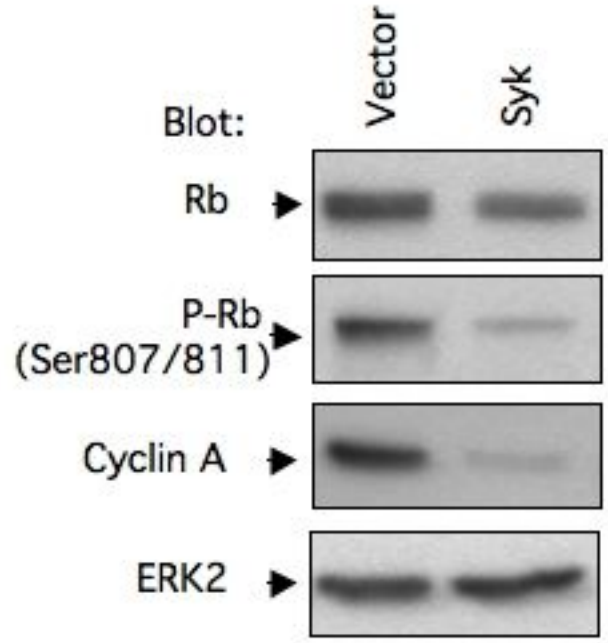
Blot:
Vector
Syk
Rb
P-Rb
(Ser807/811)
Cyclin A
ERK2

B

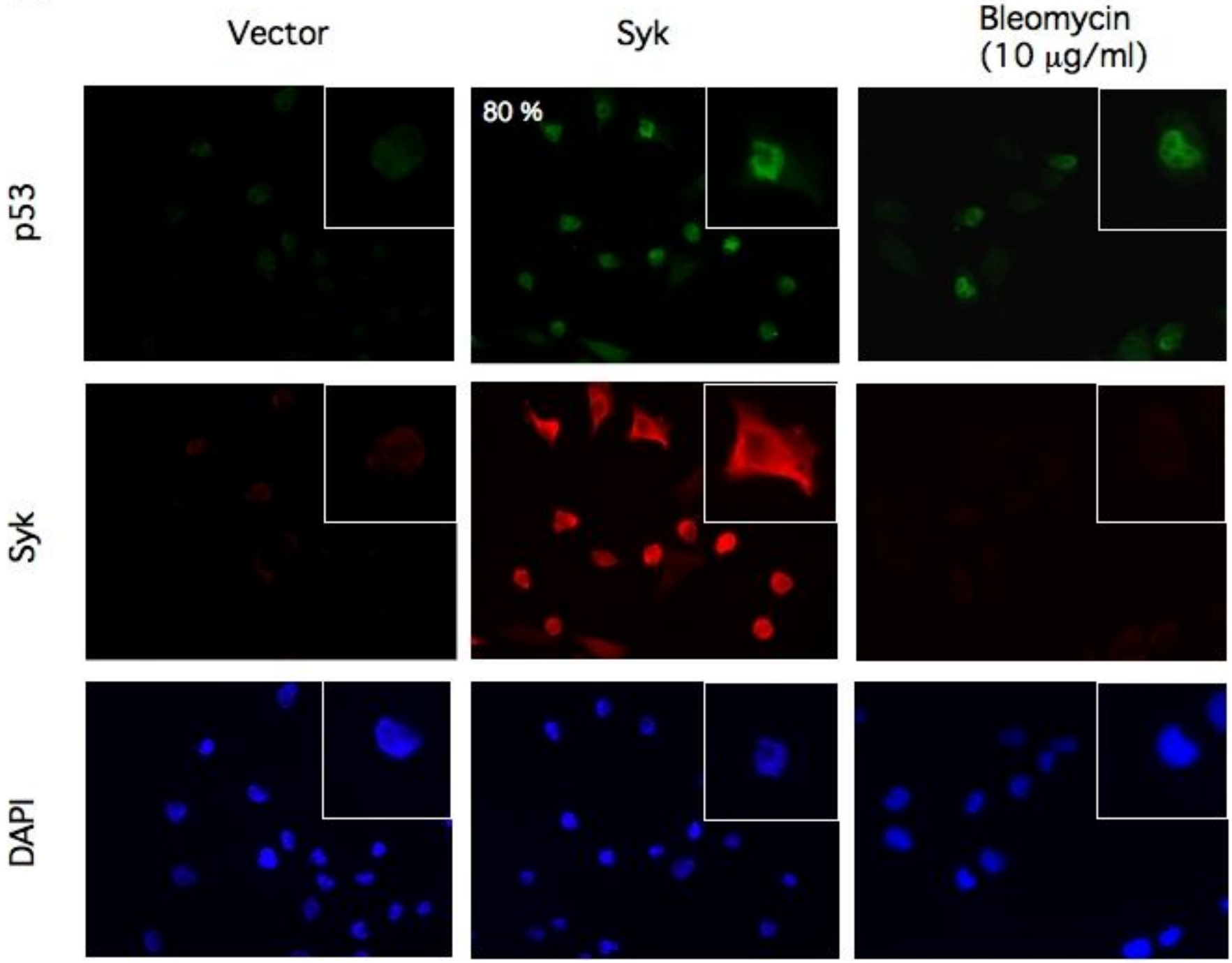
Vector
Syk
Bleomycin
(10 μg/ml)
80 %
p53
Syk
DAPI

Figure 5

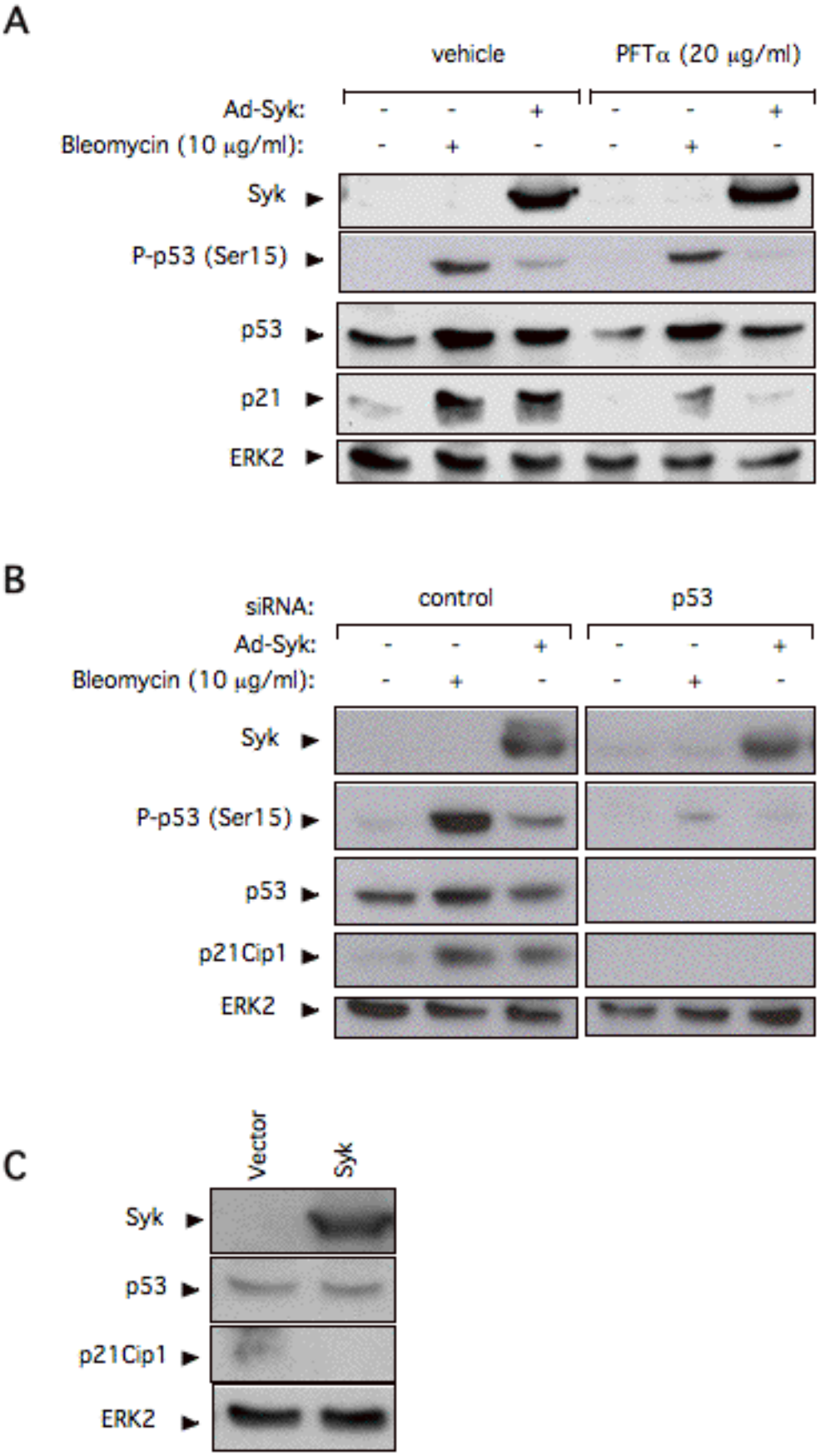
A
vehicle
PFTα (20 μg/ml)
Ad-Syk:
Bleomycin (10 μg/ml):
Syk
P-p53 (Ser15)
p53
p21
ERK2
B
siRNA:
control
p53
Ad-Syk:
Bleomycin (10 μg/ml):
Syk
P-p53 (Ser15)
p53
p21Cip1
ERK2
C
Vector
Syk
Syk
p53
p21Cip1
ERK2

Figure 6

Supplementary methods

Antibodies used in immunoblotting and immunofluorescence

Antibodies against Syk (N19 and 4D10), ERK2, p53, pRb, E2F1, survivin and p21 were from Santa Cruz Biotechnology. Phospho-Syk (Tyr352) and HP1β antibodies were from BD Biosciences and Chemicon, respectively. Phospho-p53 (Ser15), phospho-pRb (Ser807/811), JNK 1/2, phospho-JNK 1/2 and caspase 2 antibodies were from Cell Signaling Technology. Antibody against cyclin A was from Novocastra. Secondary FITC- and Texas Red-conjugated antibodies were from Molecular Probes.

Gene array analysis by Real-time quantitative PCR (Q-PCR)

Total RNA from A375 cells was isolated using TRIzol (Invitrogen). After treatment with Dnase I, 2 μg of RNA was reverse transcribed using the High Capacity cDNA Archive random priming Kit (Applied Biosystems). The expression level of 90 genes related to p53-mediated signal transduction, growth arrest and apoptosis (1, 2) was evaluated by real-time Q-PCR using an ABI Biosystems 7900HT Sequence Detector System and the SYBR Green dye detection protocol as outlined by the manufacturer (Applied Biosystems). Gene-specific primers were designed using the Primer Express software (Applied Biosystems). Relative expression level of target genes was normalized for RNA concentrations with four different housekeeping genes (GAPDH, β-actin, HPRT and ubiquitin). For each sample, C_T values for the housekeeping genes were determined for normalization purposes, and delta C_T (ΔC_T) between the mean of housekeeping genes values and target genes values was calculated. Relative expression level of target genes mRNA between mock-infected control cells (Ad-vector) and Syk-infected cells (Ad-Syk) was calculated using the formula ΔC_TAd-Syk – ΔC_TAd-vector and expressed as fold over control ($2\Delta\Delta C_T$).

Supplementary Figures:

Bailet et al. Figure S1:

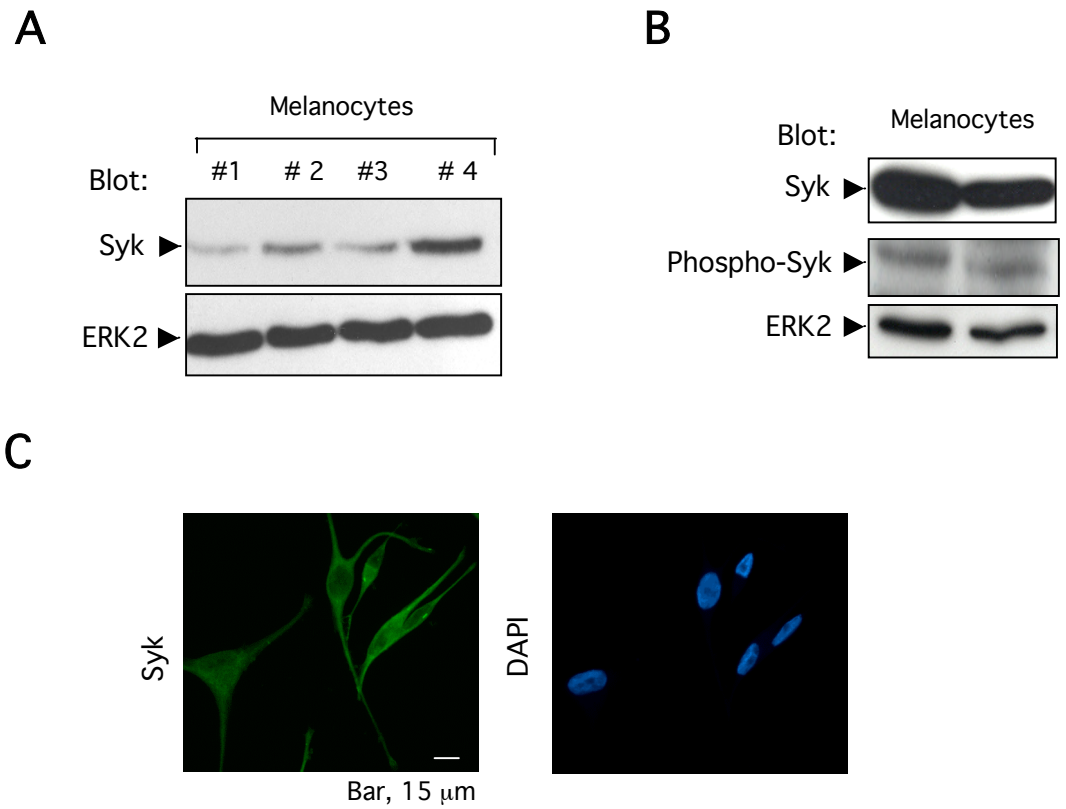

Bailet et al. Figure S2:

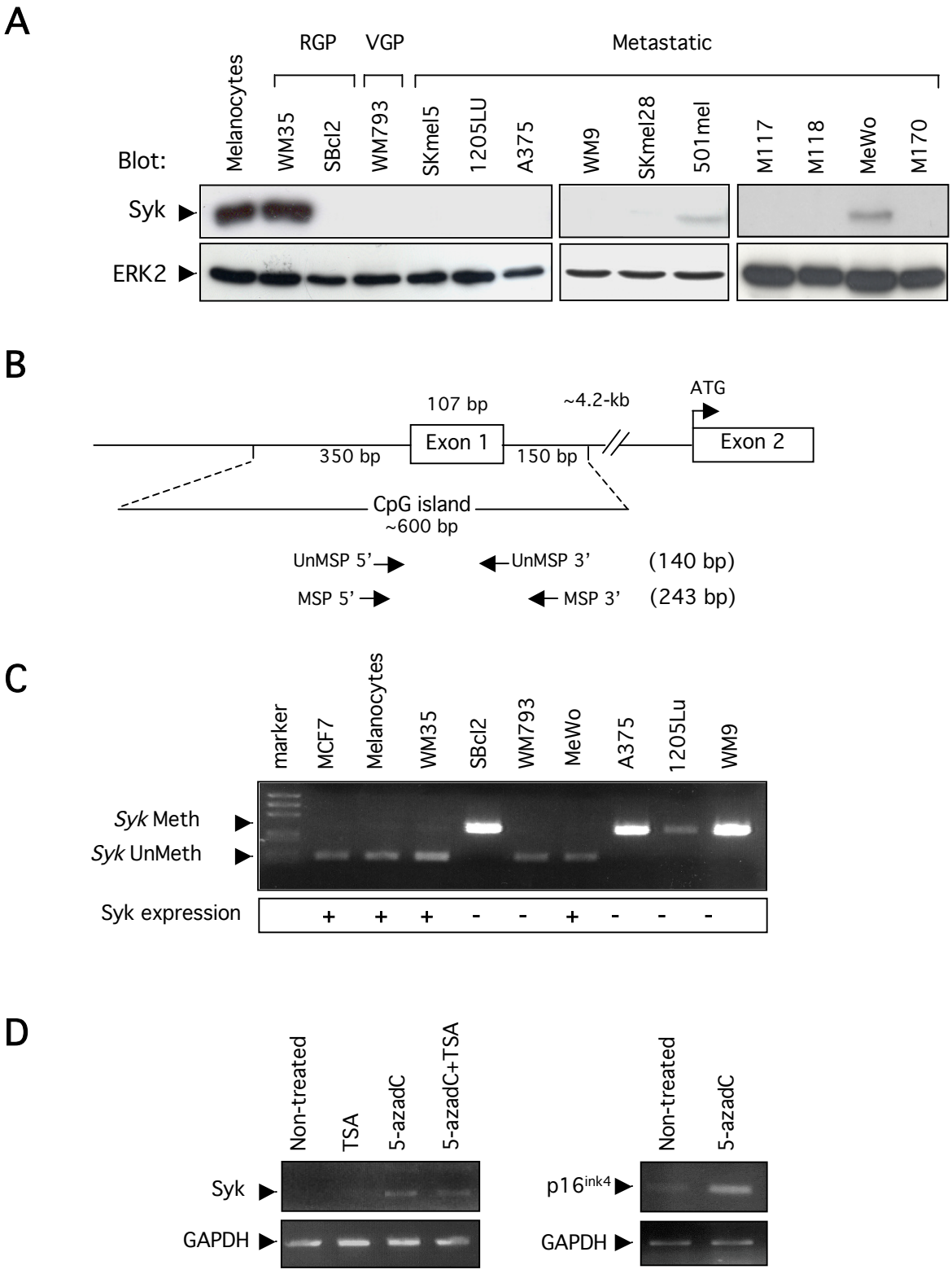

Bailet et al. Figure S3:

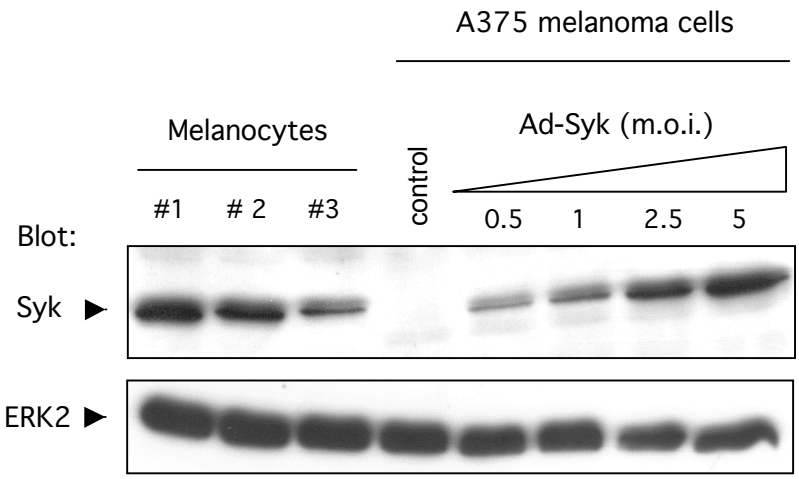

Bailet et al. Figure S4:

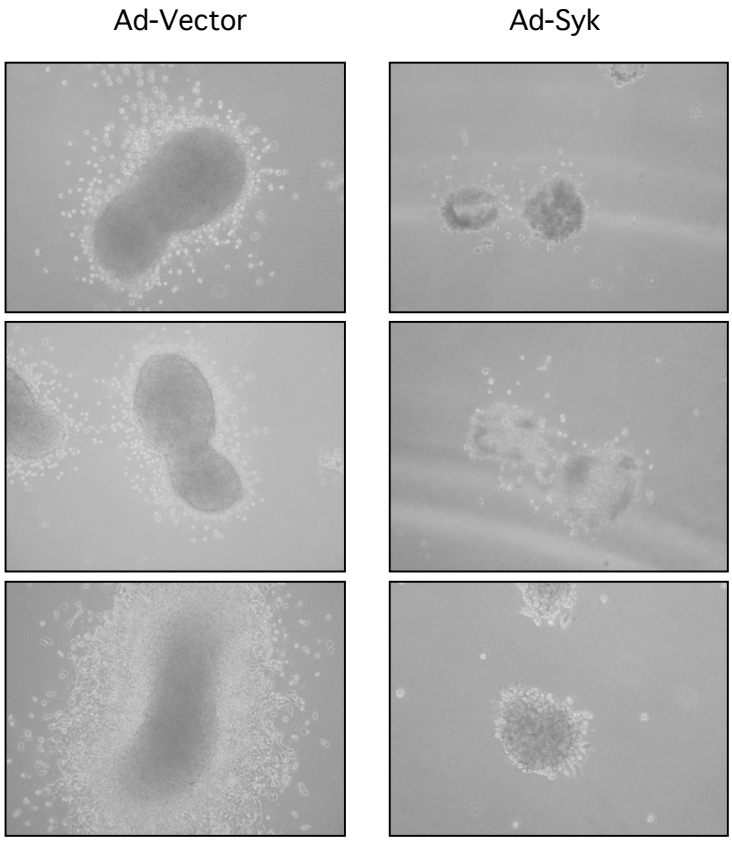

Invasion into Collagen (Day 3)

Bailet et al. Figure S5:

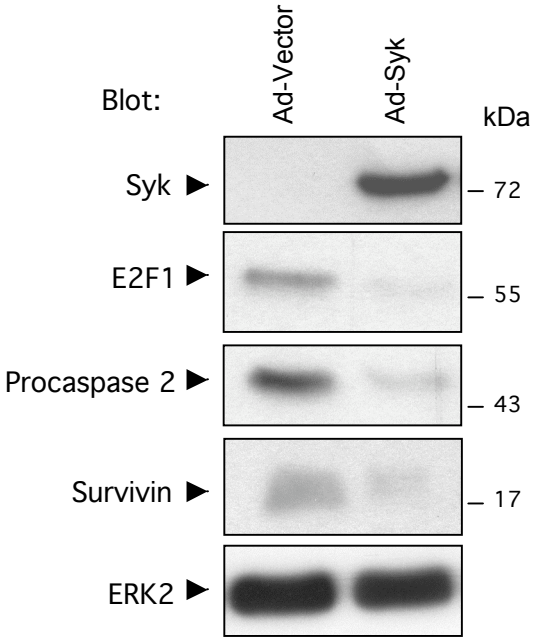

Bailet et al. Figure S6:

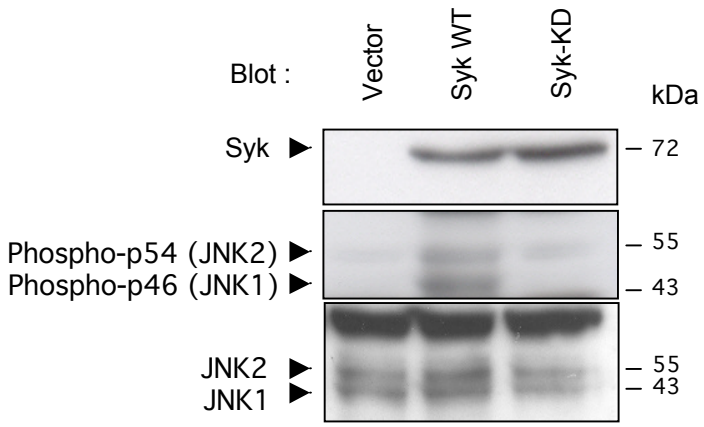

Values represent the mean of duplicates and are representative of two independent experiments.

Methylation-specific PCR (MSP) and 5-aza-2′-deoxycytidine (5-aza-dC) treatment

Genomic DNA was extracted using the DNeasy Tissue kit (Qiagen, Hilden, Germany). 1 μg of DNA was modified by sodium bisulfite treatment using the CpG genome modification kit (Chemicon International). The bisulfite-modified DNA was amplified using methylation-sensitive PCR primers as previously described in (3). To estimate the effect of demethylation on *Syk* expression, A375 cells were treated with 3 μM of the methylation inhibitor 5-aza-dC for 4 days. The cells were also treated with 1 μM of the histone deacetylase inhibitor trischostatin A (TSA) for 1 day. Cells were then collected and total RNA was prepared as above. Semiquantitative RT-PCR was carried out using conditions described previously (3). As a control for RNA integrity, the gene encoding GAPDH was amplified.

1. Vogelstein B, Lane D, Levine AJ. Surfing the p53 network. Nature 2000;408:307-10.

2. Riley T, Sontag E, Chen P, Levine A. Transcriptional control of human p53-regulated genes. Nat Rev Mol Cell Biol 2008;9:402-12.

3. Yuan Y, Mendez R, Sahin A, Dai JL. Hypermethylation leads to silencing of the SYK gene in human breast cancer. Cancer Res 2001;61:5558-61.

Supplementary figure legends:

Figure S1: *Syk is expressed and phosphorylated in normal primary melanocytes.* (A) and (B) Cellular lysates were collected from human melanocytes isolated from several donors and analyzed by immunoblotting using antibodies against Syk (A) or

Phospho specific (Tyr352) Syk (B). ERK2 was used as loading control. (C) Immunofluorescent staining of Syk in normal melanocytes. Syk was detected by staining with the polyclonal anti Syk antibody (N19). The right panel displays 4′, 6′-diamidino-2-phenylindole (DAPI) staining for nuclei.

Figure S2: *Syk is epigenetically silenced in melanoma cells.* (A) Human primary melanocytes and melanoma cell lines from various stages of progression (RGP, VGP and metastatic) were screened for Syk expression by immunoblotting. ERK2 was used as loading control. (B) Schematic map of the 5′ CpG island of *SYK*. Open boxes indicate the exons of *SYK*. Exon 1 and Exon 2 are separated by a 4.2 kb intron. The CpG island is of 600 bp in size surrounding Exon 1. Arrows: positions of primers for MSP (methylation-specific PCR). (C) MSP analysis of DNA from melanocytes and melanoma cell lines. Genomic DNA treated with sodium bisulfite was amplified using primers specific to the methylated and unmethylated forms of *SYK* DNA. Products of 243 bp and 140 bp were expected for methylated (Meth) and unmethylated (Unmeth) DNA, respectively. The breast cancer cell line MCF7 was used as control for unmethylated *SYK* DNA. The box displays the relative expression of Syk in melanocytes and cancer cell lines. (D) Restoration of Syk expression in Syk-negative cell line by 5-azadC. A375 cells were treated with or without 3 μM of the demethylating agent 5-aza-dC for 4 days and/or 1 μM of the histone deacetylase inhibitor TSA for 24 hr. RT-PCR was performed to analyze Syk mRNA expression. The right panel displays expression of $p16^{ink4}$ as positive control of drug treatment. Expression of GAPDH was used as an internal control.

Figure S3: *Analysis of expression level of exogenous Syk using adenoviral delivery.* A375 melanoma cells were infected with control adenovirus (MOI=5) or with adenovirus expressing Syk (Ad-Syk) at increasing MOI as indicated. Cells were lysed 2 days after

infection, and levels of Syk were visualized by immunoblotting and compared to those seen in three independent preparations of human primary melanocytes (#1-3). Expression of ERK2 was used as loading control. Note the similar levels of Syk in transduced-melanoma cells and melanocytes.

Figure S4: *Re-expression of Syk reduces invasion in WM793 cultured as collagen I-embedded 3D spheroids.* Preformed empty vector (Ad-vector) or Syk-infected spheroids of WM793 cells (Ad-Syk) were implanted into a gel of collagen I (0.9 mg/mL). Spheroids were incubated in growth medium for a further 72 hours and tumor cell outgrowth was visualized by phase contrast microscopy. Representative examples of vector- and Syk-infected spheroids were shown. Note the lack of cell invasion into the surrounding collagen for Syk-infected spheroids.

Figure S5: *Validation of the expression of Survivin, E2F1 and Caspase 2.* A375 cells were infected with control adenovirus or with adenovirus expressing Syk. Lysates were analyzed at day 4 post-infection by immunoblotting using antibodies against Syk, Survivin, E2F1 and caspase 2. Expression of ERK2 was used as loading control.

Figure S6: *Re-expression of Syk activates the JNK (c-Jun N-terminal kinase) pathway.* Lysates from A375 cells transduced with control adenovirus (vector) or with Syk or Syk-KD expressing adenoviruses for 3 days were analyzed by immunoblotting to determine JNK 1/2, phospho-JNK 1/2 and Syk levels.

Table S1: *Genes differentially regulated in melanoma cells infected by Ad-Syk compared to Ad-vector.* The expression level of 90 genes related to p53-mediated signal transduction, growth arrest and apoptosis was evaluated by real-time Q-PCR analysis. RNAs were prepared from A375 cells infected with control adenoviruses or

with adenoviruses expressing Syk for 4 days and then subjected to Q-PCR analysis as described in supplementary methods. Data are expressed in arbitrary units as fold change between Syk-infected cells (Ad-Syk) and mock-infected control cells (Ad-vector) and are a mean of two independent amplifications performed in duplicate.

Table 1 Genes differentially regulated in melanoma infected by Ad-Syk compared to Ad-LacZ

Name of gene	*Symbol*	*GeneBank ID*	*Fold change*
Increased with Syk expression			
Cell cycle regulation			
Reprimo, TP53 dependent G2 arrest mediator candidate	RPRM	NM_019845	2.43
Growth arrest and DNA-damage-inducible, alph	GADD45A	NM_001924	1.97
Cyclin-dependent kinase inhibitor 1A (p21, Cip1)	CDKN1A	NM_000389	2.94
Sestrin 1	SESN1	NM_014454	2.17
Mdm2, transformed 3T3 cell double minute 2, p53 binding protein	MDM2	NM_006879	1.97
DNA (cytosine-5-)-methyltransferase 1	DNMT1	NM_001379	6.25
Cell survival regulation			
Fas (TNF receptor superfamily, member 6)	FAS	NM_000043	2.09
Tumor necrosis factor receptor superfamily, member 10b (DR5)	Tnfrsf10b	NM_003842	1.94
p53-regulated apoptosis-inducing protein	P53AIP1	NM_022112	1.95
SIVA1, apoptosis-inducing factor	SIVA	NM_006427	2.77
BCL2-antagonist/killer 1	BAK1	NM_001188	2.30
Baculoviral IAP repeat-containing 4	BIRC4	NM_001167	5.59
BCL2 binding component 3	BBC3	NM_014417	1.75
BCL2-associated X protein	BAX	NM_138761	2.74
BCL2-interacting killer (apoptosis-inducing)	BIK	NM_001197	2.10
Decreased with Syk expression			
Cell cycle regulation			
CHK1 checkpoint homolog	CHEK1	NM_001274	1.87
CHK2 checkpoint homolog	CHEK2	NM_007194	2.88
Cyclin A2	CCNA2	NM_001237	1.88
Cyclin B1	CCNB1	NM_031966	2.04
Cyclin B2	CCNB2	NM_004701	2.48
Cyclin E2	CCNE2	NM_057749	1.89
Cell division cycle 2, G1 to S and G2 to M	CDC2	NM_001786	3.02
Cell division cycle 25 homolog C	CDC25C	NM_001790	2.13
E2F transcription factor	E2F1	NM_005225	6.71
Breast cancer 1, early onse	BRCA1	NM_007294	2.23
V-myc myelocytomatosis viral oncogene homolog	MYC	NM_002467	2.36
Ataxia telangiectasia mutated	ATM	NM_000051	2.16
Stratifin (YWHAS)	SFN	NM_006142	2.12
Cell survival regulation			
BCL2-antagonist of cell death	BAD	NM_004322	2.68
BCL2-like 11 (apoptosis facilitator) (BIM)	BCL2L11	NM_138621	1.77
Baculoviral IAP repeat-containing 5 (survivin)	BIRC5	NM_001168	4.75
Baculoviral IAP repeat-containing 7 (livin)	BIRC7	NM_022161	4.95
Caspase 2, apoptosis-related cysteine peptidase	CASP2	NM_032982	11.93
Nuclear factor of kappa light polypeptide gene enhancer in B-cells 1 (p105)	NFKB1	NM_003998	2.93